Optimizing Backrest Geometry to Minimize Interfacial Pressure Concentrations in the Mid-to-Lumbar Region During Leg Press Resistance Training

Journal Article

Author(s):
Castonguay-Siu, Vincent; Taylor, William R.

Publication date:
2022-03

Permanent link:
https://doi.org/10.3929/ethz-b-000529850

Originally published in:
Journal of Biomechanical Engineering 144(3), https://doi.org/10.1115/1.4053133

Optimizing Backrest Geometry to Minimize Interfacial Pressure Concentrations in the Mid-to-Lumbar Region During Leg Press Resistance Training

Vincent Castonguay-Siu
Institute for Biomechanics,
ETH Zürich,
Zürich 8093, Switzerland

William R. Taylor[1]
Institute for Biomechanics,
ETH Zürich,
Zürich 8093, Switzerland
e-mail: bt@ethz.ch

The leg press is a resistance training (RT) exercise common to both weight- and powerlifting, where spine-related injuries remain prevalent. Here, the elevated loading has the potential to result in increased pressure on vertebral bodies and introduce the risk of spinal injury. This study, therefore, investigates back interfacial pressure under leg press loading conditions and offers design recommendations to minimize spatial pressure concentrations. A pressure mat was used to assess the back-backrest interfacial pressure distribution of 15 subjects executing RT leg-presses at 50% body weight, over 16 different back-support geometries. Real-time forces, knee angles, and pressures were captured. The resulting data show that more prominent (≥2.1 cm) back-supports, positioned 19 cm above the seat pan typically produced greater peak pressures (41.8 ± 7.2 kPa). Conversely, less prominent supports (∼0.7 cm) generally achieved lower peak pressures (with greater distribution). Our data suggest that the most prudent choice for fixed-shape backrests to best distribute interfacial pressure on leg-press devices is to incorporate shallow convex supports (∼0.7 cm) and locate them away from *P = 19 cm. The result is surprising as this prominence location is a common ergonomic feature. If an adjustable backrest is considered, peak pressures may be reduced by up to 26 ± 8% (9.7 ± 3.1 kPa) compared to flat geometries.* [DOI: 10.1115/1.4053133]

Keywords: low back pain, pressure distribution, backrest pressure, leg press, body/seat interaction

Introduction

The lifetime prevalence of nonspecific low back pain (LBP) is estimated to be between 60% and 70% in industrialized countries and remains one of the most common reasons for medical consultations [1]. Although the underlying etiology of LBP remains unknown, resistance training (RT) has been shown to be an effective therapeutic modality in the treatment of nonspecific LBP [2–4]. However, due to the elevated loads employed during RT exercises, there is inherent potential to aggravate existing LBP or to induce acute injury, potentially resulting in future chronic LBP. This is particularly true for exercises in which the load is supported by the upper body while the body's center of mass (CoM) is rotated anteriorly (e.g., during squats or deadlifts), as such positions often result in increased compressive forces and bending moments around the lumbar spine. As these are fundamental exercises in both weight- and powerlifting, it comes as no surprise that acute spine-related injuries remain frequent in these sports [5]. Due to a combination of factors, such as inherent body-core stability during the exercise, more targeted musculature engagement, and increased spinal support (offered by the seated position), the leg press exercise has risen in popularity as an alternative means of lower body RT. However, at lower movement velocities, the maximal output forces that may be achieved on a leg press can actually exceed those attained during a squat [6]. Here, the seat pan and backrest geometries are thought to play a key role in supporting the back and guiding load distribution [7]. Internally, anterior-posterior vertebral shear will be generated not only from active musculoskeletal forces but also from the interaction between the backrest and each individual's spinal anatomy.

Much work has been conducted investigating both interfacial force/pressure distribution and spine biomechanics for working postures, particularly for seated positions [8–11]. Many of these works have supported the development of ergonomic chairs and vehicle seats intended to reduce musculoskeletal stress and lower the incidence of chronic LBP [12–14]. As a result, curved prominences in office chairs at a height of approximately 19 cm above the seat pan are commonplace [15]. However, few such studies, if any, have been extended to examine the interface loading conditions associated with RT equipment. Through an improved understanding of the interfacial pressure conditions during the leg press, it may be possible to target a reduction in vertebral shear by optimizing the backrest to distribute interfacial pressure more evenly, thereby reducing the risk of spinal injury. However, it remains unknown whether any single backrest geometry can universally minimize pressure peaks across the back during leg press RT.

As such, this work concerns itself with two primary objectives. The first is to investigate the dynamic interfacial pressure distribution between the user and the backrest under leg-press loading conditions. The second is to offer technical recommendations for the development of backrest profiles designed to optimize the interfacial pressure to distribute loading more evenly along the spine and potentially minimize shear stress between vertebrae.

Materials and Methods

Participants. Fifteen healthy subjects ranging in resistance training experience (7 male/8 female; age: 25 ± 6 years [21–45], height: 1.72 ± 0.08 m [1.59–1.85], mass: 69 ± 11 kg [53–86], and body-mass index: 23 ± 2 kg/m^2 [19–27]) took part in this study. Subjects were convenience sampled based on interest and availability. No subject reported any spinal or lower body musculoskeletal disorders. All subjects provided written informed consent before participating in this study, which was approved for publication by the institutional ethical review board under application number 2021-N-156.

Leg-Press Set-Up. A prototype version of the DD System Pro (Dynamic Devices AG, Zürich, Switzerland) was retrofitted with a custom-built backrest that facilitated the geometric adjustment of the backrest support (Fig. 1). The DD System Pro (previously Allegro) [16–18] is characterized as a closed kinetic chain dynamic leg-press, featuring an interactive training system, and independently force-controlled pedals [17]. Loading is achieved through a leverage-based system powered by pneumatic artificial muscles (Fluidic Muscle, Festo AG), where a force-pressure-length mapping scheme ensures closed-loop real-time force control. The rotary encoder at the fulcrum of the pedals registers the machine angle (precision < 0.1 deg), which is converted to anatomical knee angles based on individual calibrations. The system is able to generate forces ranging from 0–1400 N per leg [19,20], quantified through a continuous resolution scale (precision < 0.1 N), and a 2% full-scale accuracy [16,21]. Footplate force is collected through a combination of onboard pressure valves and sensors.

Experimental Design. The seat-pan to backrest angle was kept fixed in the most upright position possible (104 deg), where the knee angle was defined as the angle formed by the projected

[1]Corresponding author.
Manuscript received March 4, 2021; final manuscript received November 17, 2021; published online January 21, 2022. Assoc. Editor: Anton E. Bowden.

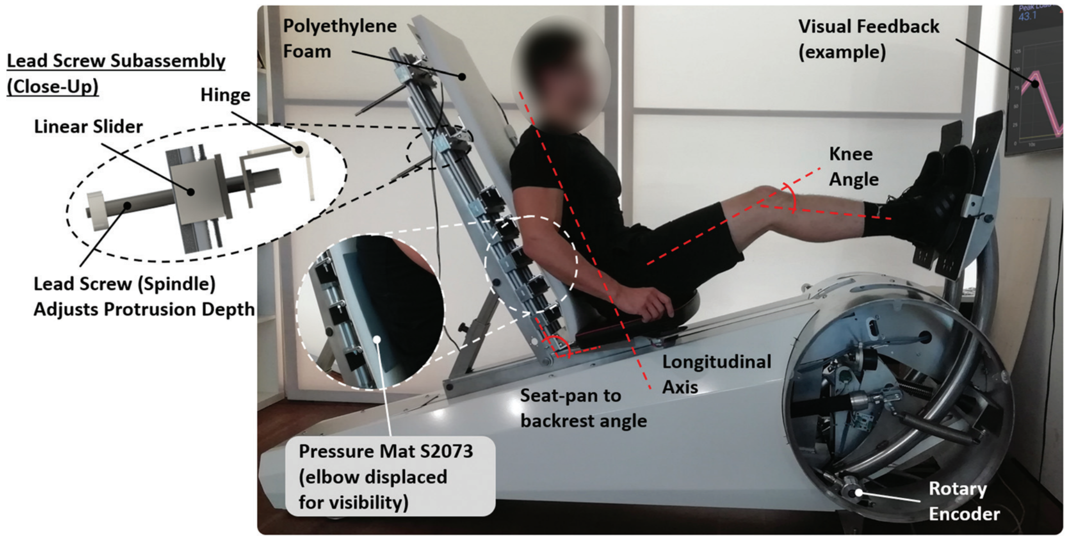

Fig. 1 Subject performing a test on the DD System Pro-instrumented with a pressure mat and retrofitted with a custom-built backrest. The sliding lead screw subassemblies are used to adjust the backrest profile by shaping the flexible surface to form a smooth continuous backrest interfacing with the subject's back.

longitudinal axes of the femur and the tibia. Here, the flexed position referred to a knee angle of 90 deg, with 0 deg considered fully extended. The System Prowas calibrated for each individual to allow the determination of the subject-specific anatomical knee angles. Calibration was performed by having each subject position undergo knee flexion at specified angles (0 deg, 30 deg, 45 deg, 60 deg, 90 deg) while the System Prorecorded the associated machine angle for the encoder. During the exercise, a visual interface provided the subject with real-time feedback pertaining to target and actual (interpolated) knee angles. Potential angular deviations arising from plantarflexion were minimized by allowing the footplates to freely pivot about a hinge situated at their respective centers.

Adjustable lead screw subassemblies enabled prominences that produced variable backrest support depths and positions (height from seat-pan). This setup permitted backrest profile continuity for various back support geometries, which were defined by the vertical position and depth of the center of the curved prominence. A constant support slope was maintained by setting the adjacent adjustment points 0.7 cm less than the depth of the central prominence. This resulted in linearly decreasing depths, beginning from the trial support depth, and ending at the reference depth of the backrest.

A total of 15 different backrest configurations were tested (Position, $P = 4.6$, 9.4, 19.0, 28.4, or 33.2 cm; Depth, $D = 0.7$, 1.4, or 2.1 cm), with all test sessions additionally including the neutral geometry (flat backrest profile, $D = 0$ cm). The order in the backrest configurations were tested was computer-randomized for each participant. A protocol comprising of a set of 10 repetitions, consisting of 4 s of eccentric and 2 s of concentric exertion, resulted in 60 s trials. Trials were performed using 50% of the subject's body weight per leg. At least 3 min of rest was provided between trials, and test sessions were constrained to avoid muscular fatigue. Generally, not all backrest configurations could be investigated within a single session, with subjects typically achieving 9–10 configurations per session, since the neutral geometry was also tested five times to obtain a reliable control and quantify intrasubject variability. Eight subjects (4m/4f) made themselves available on multiple occasions to allow the complete range of configurations to be investigated (termed "repeat subjects").

Subjects performed two unrecorded practice sets to allow accustomisation. During testing, the subject was instructed to be seated, firmly press their lower back against the backrest, place their hands in a comfortable position (where they would remain), and perform each trial repetition in a single, fluid motion. Here, the trial began and ended in the near-extended position (~5 deg) to avoid subject's locking their knees, and involved flexing to a knee angle of 90 deg. Loading was kept constant throughout the protocol such that muscular tension was maintained for the duration of the trial.

Data Collection and Analysis. Subject knee angles ranging from ~5 deg to ~90 deg were measured on a continuous resolution scale through the system's rotary encoders. Force and knee angle data were sampled at 200 Hz. Pressure distribution was assessed using a pressure sensor mat (S2073, pliance-××32 Expert Version 20.3.36, Novel GmbH, Munich, Germany), which comprised of an array of pressure-detecting elements (16×16 sensors, $226 \times 226\,\text{mm}^2$) with an associated spatial resolution of 1.4 mm [22]. Each element recorded pressures ranging from 2–120 kPa, at a resolution of 1 kPa, sampled at 50 Hz.

Force, angle, and pressure data were processed in MATLAB (MathWorks Inc., Natick, MA). Preprocessing comprised of down-sampling System Prodata to match the sampling rate of the pressure mat, filtering both datasets using a 3rd order low-pass Butterworth filter, and synchronizing the data. As the concentric and eccentric portions of the exercises differed in duration, it was possible to empirically determine that mean backrest pressure reached its maxima when the legs were in the extended state. As such, the data sets were synchronized by matching the pressure maxima to knee angle minima (Appendix A: Data Processing and Analysis, Fig. 5). Data from the five best consecutive repetitions were then cycle-averaged, while the remainder was truncated. The cycle-averaged peak (per sensor element) and mean spatial pressures of the backrest pressure distribution were computed (Appendix B: Example Data, Fig. 6). The array coordinates of the element exhibiting the greatest peak pressure were then associated back to physical coordinates. This was done for each back-support geometry considered for each subject. Positional shifts of the pressure peaks that arose from altering the backrest profile were collected, averaged across subjects, and plotted as a function of support geometry.

To assess intrasubject variability, pressure distribution characteristics for each subject were extracted from the individual datasets of all control geometry trials ($N = 5$, flat backrest profile) by computing the subject-specific median peak values and interquartile ranges. These subject-specific medians were then used to normalize pressure values for each subject. To assess intersubject

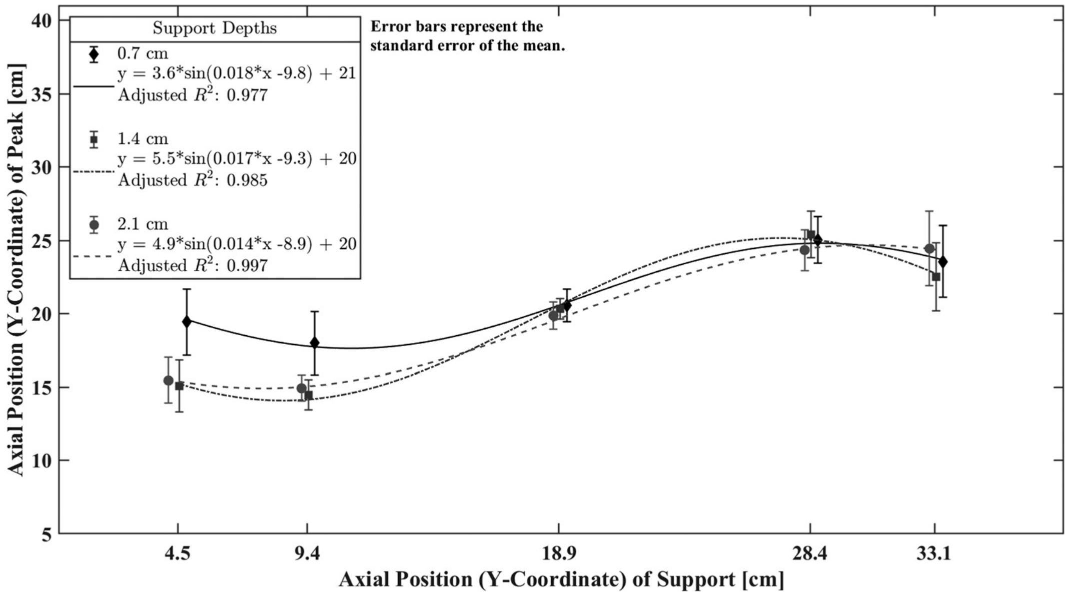

Fig. 2 Axial position (Y-Coordinate of backrest) of the peak pressure as a function of back support geometry (presented with slight offsets for clarity of data). Data depicts a sinusoidal pattern for all three support depths considered. The axial position of the pressure peak is bound within a region of approximately 11 cm, despite the support positions ranging from 4.5 cm to 33.1 cm.

variability, these normalized pressures were then amalgamated for all subjects. Finally, to evaluate the effect of backrest geometry on peak pressure, the mean resultant peak pressure (normalized) for any given backrest geometry was tested against the control using the Wilcoxon test, with results considered to be statistically significant when $p < 0.05$. Here, the test statistic could not be assumed to be normally distributed due to the limited number of participants.

Subjective information on the most and least comfortable configurations was collected for the nine central backrest configurations (Position, $P = 9.4$, 19.0, 28.4 cm; Depth, $D = 0.7$, 1.4, or 2.1 cm) and compared with the magnitudes of the normalized peak pressures of the control configuration to determine the relationships between relative comfort and pressure distribution. Subjects were prompted after each relevant test to assess if the last backrest profile was the most/least comfortable tested thus far. Responses were manually recorded by the investigator. All statistical analyses were performed within MATLAB.

Results

Peak Pressure Positioning as a Function of Support Geometry. Unsurprisingly, for tests performed under the control (flat) backrest profile, pressure peaks remained central in the mediolateral direction. Similarly, no correlation was found between the vertical position of the pressure peak (y_p) and subject height

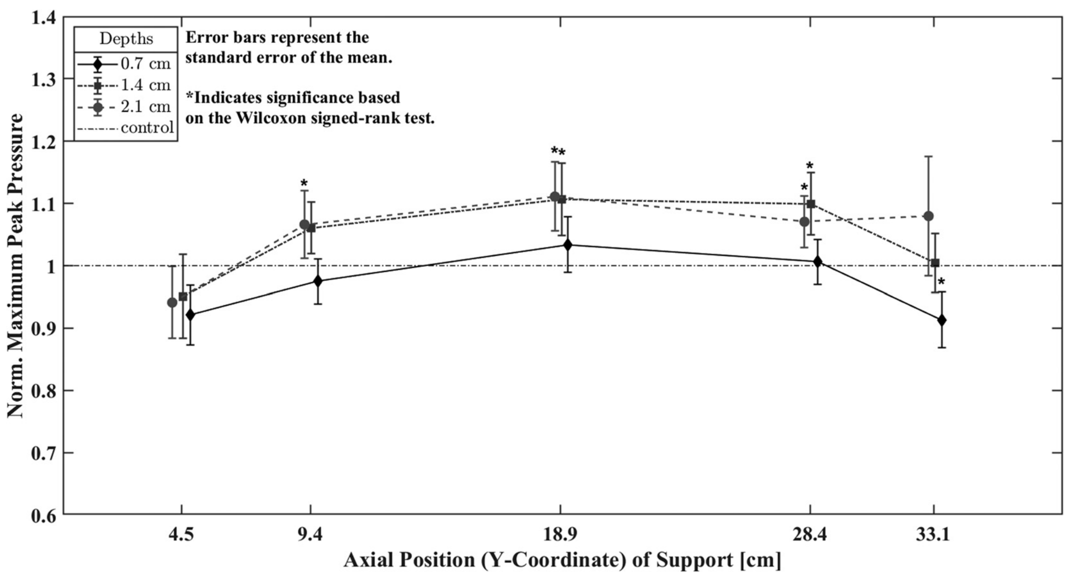

Fig. 3 Mean intersubject normalized peak pressure plotted as a function of the axial position (Y-Coordinate of backrest – presented with slight offsets for clarity of data) of the support. Interfacial peak pressure attains a relative maximum when supports are positioned at approx. $P \approx 19$ cm. Centrally positioned supports exhibited increased peak pressure whereas supports positioned at the extremities reduced the interfacial peak pressure.

($R^2 = 0.05$; $N = 15$). The intersubject mean of the individual median peak pressures, $\bar{\bar{p}}$, and their associated interquartile ranges, $\overline{IQR_p}$, was 37.7 ± 5.7 kPa. The mean location of the intersubject median peak pressures for the control profile was $\bar{\tilde{y}}_p = 20.9 \pm 5.4$ cm. For backrest profiles that included a back support, the location of the pressure peak and the position of the support prominence appeared to share a sinusoidal relationship for all support depths considered (Fig. 2). The mean location of the pressure peak remained constrained to an 11 cm region ($\overline{y_p} \in$ [14.4, 25.4] cm), despite the position of the back-supports ranging from 4.5 to 33.1 cm. While data collected with the back-support positioned at the vertical extremities ($P = 4.5$ cm and $P = 33.1$ cm) contained greater variation, the strength of the sinusoidal models remained consistently high, achieving a coefficient of determination of $R^2 = 0.997$ for a supported depth of $D = 2.1$ cm (Tables 1 and 2).

Peak Pressure Magnitude as a Function of Back Support Geometry. On average, subjects presented normalized pressure distributions that peaked toward $P \approx 19$ cm from the seat-pan (Fig. 3). Back support geometries with the smallest prominences resulted in lower normalized peak pressures than the two greater support depths considered, regardless of the position of the support. Ten backrest profiles resulted in higher mean intersubject normalized peak pressures ($\overline{p_n}$) than those obtained for the neutral control profile (effect size: 0.4%–11.1%), with five reaching significance based on the Wilcoxon test (Appendix D: Mean Normalized Peak Pressure for Various Backrest Geometries, Table 3). Five back-support geometries achieved lower peak pressures (2% - 9%), but only one attained significance. Here, the reduction in peak pressure associated with backrest profiles exhibiting the lowest peak pressure on an individualized basis achieved a mean reduction of 26% ±8% for the repeat subjects. However, all configurations exhibited relatively large standard deviations, suggesting considerable intersubject differences in pressure distributions.

Dis-/Comfort and Peak Pressure. There was no clear trend in subjective comfort in terms of position and depth (Fig. 4(*a*)). When considering the backrest profiles containing a centrally positioned back-support ($P = 9.4$, 18.9, or 28.4 cm), those that produced the greatest reduction in peak pressure relative to the neutral profile were located at $P = 9.4$ cm and $P = 28.4$ cm, and typically had a less prominent support depth (Fig. 4(*b*)). Conversely, back support depths equal to or greater than $D = 1.4$ cm, positioned at the center of the tested range ($P = 18.9$ cm), were most likely to result in both increased discomfort (Fig. 4(*c*)) and higher peak pressures (Fig. 4(*d*)). For configurations containing a centrally positioned back-support, the peak pressures ($\overline{p_n} \pm \sigma_{\overline{p_n}}$) associated with the subject-specific backrest profiles that resulted in the greatest subjective comfort, lowest peak pressures, and greatest peak pressures were found to be $\overline{p_n}_{\text{comfC}} = 1.01 \pm 0.13$, $\overline{p_n}_{\text{minC}} = 0.87 \pm 0.08$, and $\overline{p_n}_{\text{maxC}} = 1.34 \pm 0.1$, respectively.

Discussion

The elevated loads employed during leg press training induce severe interfacial loading conditions between the user's back and the seat, inherently introducing the potential for injury, which may be exacerbated through unfavorable backrest geometries. As such, here, we have investigated the viability of altering the backrest geometry to optimize interfacial pressure distribution, plausibly reducing the risk of spinal injury during leg press resistance training. The results of this study are now able to demonstrate that backrest geometry and prominence location play a considerable role in the interface pressures during leg press exercises, but not in a manner that would have been expected from more traditional, static, seating ergonomic designs.

Pressure Peak as a Function of Support Geometry. Results collected from the repeated tests ($N = 5$) of all 15 participants for the control backrest profile suggest no correlation between the position of peak pressure and subject height. While the absence of such a correlation is unsurprising for the mediolateral axis, our results may be counterintuitive axially, as one may expect stature

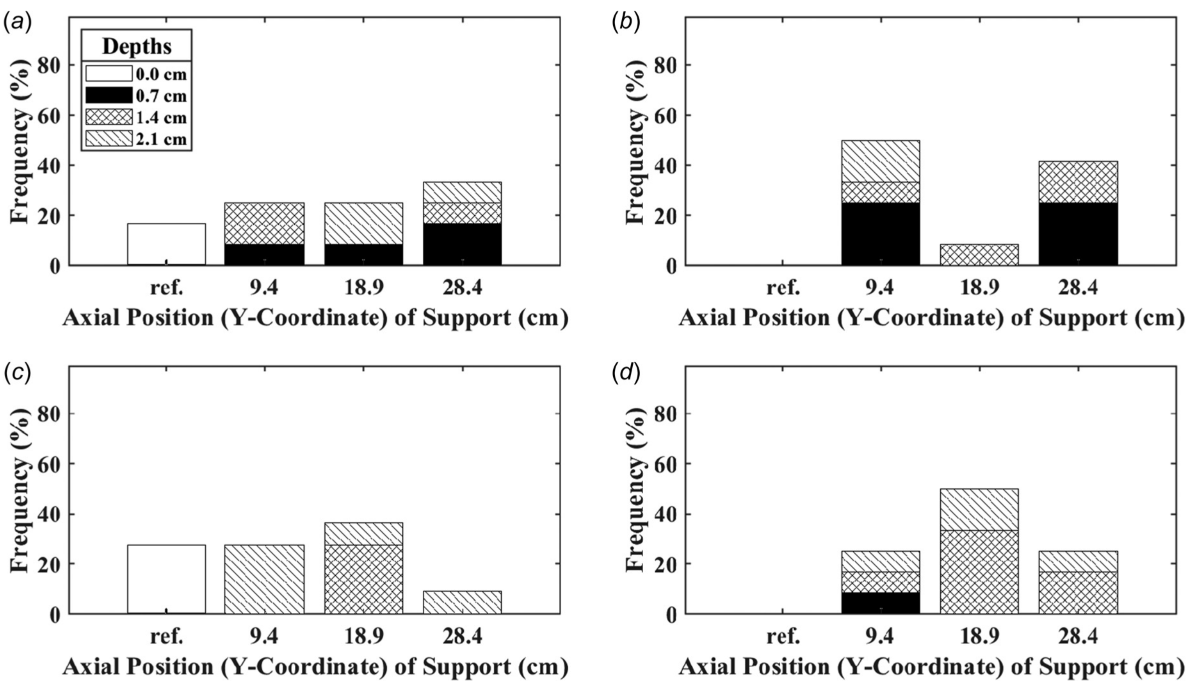

Fig. 4 Frequency (%) that a backrest support geometry resulted in the: (*a*) greatest self-reported comfort, (*b*) lowest peak pressure, (*c*) greatest self-reported discomfort, and (*d*) greatest peak pressure for the inner range of tested support positions. If the neutral backrest profile was either reported as the least comfortable support geometry or the subject perceived no significant difference between tested geometries, the position/depth of the support was reported as "0" cm.

to dictate the position/height of spinal curvature. However, this finding does fall in line with previous work describing the absence of a relationship between stature and positional preferences for back supports [15]. This may suggest that individual differences in spine geometries and posture are sufficiently large to overshadow overarching trends originating from differences in height. Here, greater sample size is likely required to see the emergence of such trends.

Our data suggest a strong relationship between the back-support position and the location of the pressure peaks (Fig. 2). While it may be intuitive to assume that the pressure peaks would gravitate toward prominences directly interfacing with the subjects' back, instead we observed that the relationship between the position of the pressure peak and the location of the support prominence presents a sinusoidal shaped curve for all support depths. Although the data exhibited high intersubject variability, the high coefficients of determination, alongside excellent repeatability across support depths, indicate that, despite the wide range of axial support positions considered, the location of the interfacial peak pressure remains bound to a region of approximately 11 cm. These data suggest that while altering the backrest profile can modulate the locations of peak interfacial pressure to a limited extent, anatomy, posture, and required muscular forces likely govern the general regions where the maximum interfacial pressure occurs during this exercise.

When peak pressure is presented as a function of back support position (Fig. 3), it becomes clear that centrally positioned prominences result in greater peak pressures relative to the control geometry, as eight (of nine) of these backrest profiles resulted in peak pressure increases. Of these eight, five were found to increase peak pressure to a significant degree based on the Wilcoxon test. Conversely, back-support prominences positioned at the extremities of the tested range were associated with a decrease in peak pressure. Five (of six) of these geometries showed decreased peak pressures, with one achieving a significant reduction. The limited number of support geometries found to significantly reduce peak pressure could be attributed to the high degree of intersubject variability, which could also account for the unexpected rise in peak pressure associated with the back-support positioned at $P = 33.1$ cm for a supported depth of $D = 2.1$ cm. This specific support geometry saw the greatest standard deviation in peak pressure by approx. 50% ($\overline{\sigma_{pn}} = \pm 0.32$).

Interestingly, while backrest profiles associated with the largest reduction in peak pressure were the ones that contained the least prominent back-support ($D = 0.7$ cm), backrest profiles that increased peak pressure to a significant extent contained larger prominences ($D = 1.4$ cm or 2.1 cm). Furthermore, geometries containing the centrally-positioned shallow back-supports ($D = 0.7$ cm) were found to increase peak pressure to a lesser extent relative to the greater prominence depths tested (Fig. 3). Thus, keeping the back-supports relatively shallow appears to not only be the most optimal choice, but also the most prudent. As a result, changes in both the location and magnitude of the peak pressure clearly indicate that altering the backrest profile is able to modify the overall interfacial pressure distribution. What remains unknown from this data, however, is the role that changing interface pressure distribution plays on the internal musculoskeletal loading conditions, including the muscle and joint contact forces surrounding the spine [23].

Comfort/Discomfort and Peak Pressure Minimization/Maximization. When considering subject-specific backrest profiles limited to centrally positioned prominences, the greatest mean reduction in peak pressure was ~13%, which still fell short of attaining significance. However, this individualized approach remains a considerable improvement relative to the reduction attained using a one-size-fits-all approach (~2%), i.e., for any single backrest geometry. Interestingly, it was found that subjective comfort was not a general predictor of a reduction in peak pressure (Figs. 4(*a*) and 4(*b*)). However, centrally-positioned prominent back-supports frequently induced both subjective discomfort (Fig. 4(*c*)) and increased peak pressure (Fig. 4(*d*)). Here, the greater agreement between discomfort and increased peak pressure, compared to comfort and reduced peak pressure, is likely due to several factors. First, the subject-specific geometries that increased peak pressure did so by ~34%, whereas the subject-specific geometries that could reduce peak pressure only achieved a pressure reduction of ~13% on average. This nearly three-fold difference, combined with the intrinsic challenge associated with memorizing and comparing the sensation of subjective dis/comfort [24], likely resulted in subjects more easily distinguishing backrest profiles that induced greater discomfort than profiles that resulted in slightly increased comfort.

Interestingly, the vertical position of the back-support most frequently associated with discomfort appears to conflict with observations in office chairs. Here, Coleman et al. found that office workers most favored back supports placed at a vertical distance of ~19 cm from the seat's surface [15]. However, our data suggest that this is the least comfortable backrest support position during leg-press RT. This discrepancy likely arises from the nature of the application. While office chairs are intended for prolonged static usage, leg press training devices are intended for brief but dynamic and loaded applications. It is important to note that the peak pressures observed within our study were typically obtained as the subjects' legs approached the extended state (~5 deg), immediately preceding eccentric exertion – a position that is dissimilar to seated postures in office chairs. Moreover, the high external forces that push the subject toward the backrest – as well as the associated internal musculoskeletal loads – likely result in a change in spinal curvature, known to be dependent on lower limb positioning [25] and pelvic rotation [26,27]. It should therefore come as no surprise that the vertical position of the back-support prominences that maximizes comfort also deviates between these applications.

The prominence of the back-support favoring a reduction in interfacial peak pressure ($D = 0.7$ cm) was similar to the optimal prominence determined by Guo and coworkers for vehicle seats [28]. Their data suggest a supported depth of $D = 1.0$ cm was ideal for minimizing both contact pressure and stress on the intervertebral disks of the lumbar spine. The trend of increasingly aggressive support depths resulting in increased pressure conditions observed in our study paralleled Guo's work in that increasing the depth beyond $D = 1.0$ cm resulted in an increase in both contact pressure and modeled stress for intervertebral disks [28].

Limitations and Sources of Uncertainty. Our results have conceivably been influenced by the effects of muscular fatigue between trials and learned behavior within and between sessions. While conditioned individuals could be expected to demonstrate greater fatigue resistance [29,30] and control, in terms of both position and force [31,32], our less-conditioned participants did indeed fatigue earlier, in addition to exhibiting more pronounced learned behavior during sessions. Thus, we could expect increased variation in data collected from less-conditioned individuals due to the combined effects of fatigue and learned behavior. However, this variation could reasonably be expected to be evenly spread throughout the data due to the randomized order of the trials. As the recline angle is known to play a role in force distribution along with the backrest and seat-pan, the fixed seat-pan to backrest angle considered here may limit the practical applicability of this study [7]. Finally, the convenience-sampled subjects may have introduced a volunteer bias and led to a higher likelihood of the participants being university-aged and potentially exhibiting greater resistance to muscular fatigue relative to a general population.

It is unclear that the location of the absolute pressure peaks was captured due to the limited size of the pressure mat. However, as the position of the pressure peak remained within a band of 11 cm (Fig. 2), and therefore fully within the capture area, this limitation is unlikely to have resulted in overlooked data. However, whether the application of more prominent back-support depths would have moved the peak pressures to locations outside of the pressure mat capture region remains unclear. The second source of uncertainty involved the detection of nonspinal bony prominences, such as the iliac crests, which occurred when testing backrest profiles where the support was situated at the lowest vertical position ($P = 4.5$ cm) for taller individuals ($H \gtrsim 1.70$ m). This likely contributed to some of the variation seen in both the magnitude and position of mean intersubject peak values associated with this support position.

Conclusions

The minimum normalized peak pressure ($\overline{p_n}_{\min} = 91 \pm 15\%$ of control) occurred when the backrest support was small and positioned at the upper extremity of the vertical range tested. Generally, normalized peak pressure increased when back supports were positioned at $P \approx 19$ cm from the seat-pan, regardless of prominence, with the maximum ($\overline{p_n}_{\max} = 1.11 \pm 0.19$; $\overline{p}_{\max} = 41.8 \pm 7.2$ kPa) occurring when the support was most prominent at this position. Given the large intersubject variations it seems difficult to recommend "one-size-fits-all" backrest profiles. Nonetheless, when designing static backrests intended for leg press loading conditions, it is advisable to avoid positioning supports at $P \approx 19$ cm and to limit back support prominences to depths of ≤ 0.7 cm, as lesser prominences exhibited smaller peak pressures throughout the entire vertical range considered. Additionally, it seems ill-advised to use support geometries similar to those applied in office chairs since these were shown to result in increased peak interface pressures – probably as a result of the different postures and high loading of the lower extremities. While subjects did not typically identify the geometry that most greatly minimized peak pressure as the most comfortable, they more frequently identified the least comfortable backrest profile as the one that coincided with the greatest peak pressures.

Although a fixed backrest may be able to reduce interfacial peak pressure, an adjustable backrest remains most favorable for peak minimization. While improperly adjusted backrests may increase localized pressure to a greater degree than fixed backrests, modifying support geometries to suit the individual is able to result in significant reductions in interfacial peak pressure.

Acknowledgment

The authors would like to thank Dynamic Devices AG, specifically Dr. Max Lungarella and Raja Dravid, for the technical support and guidance provided throughout.

Appendix A: Data Processing and Analysis

The flowchart below outlines the steps involved in processing raw data (1st cycle processing) and the steps involved in analyzing key values to establish general trends (2nd cycle processing).

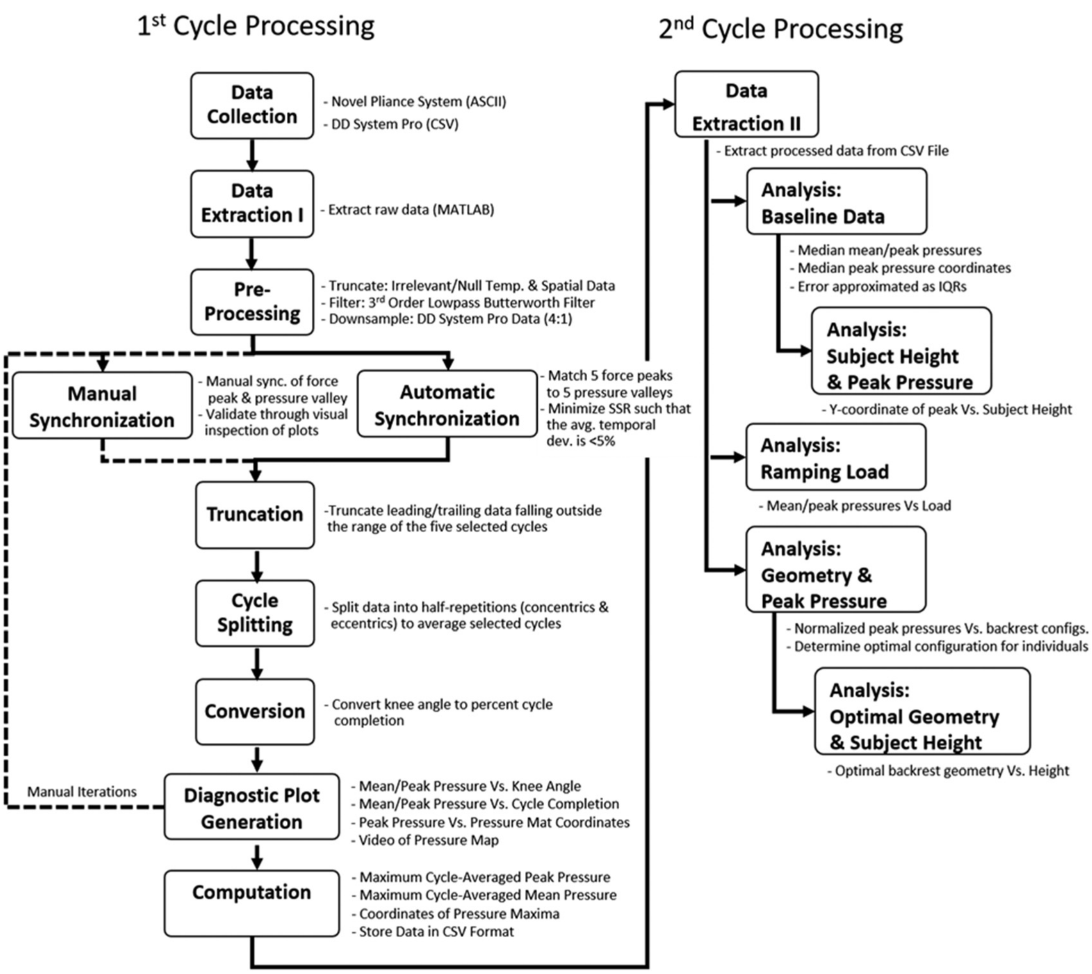

Figure 5 Steps involved in processing raw data (Cycle 1) and analyzing trends (Cycle 2). Raw pressure data originates from the Novel Pliance S2073 pressure mat and its associated hardware/software. Raw foot pedal force and knee angle data originates from the DD System Pro.

Appendix B: Example Data

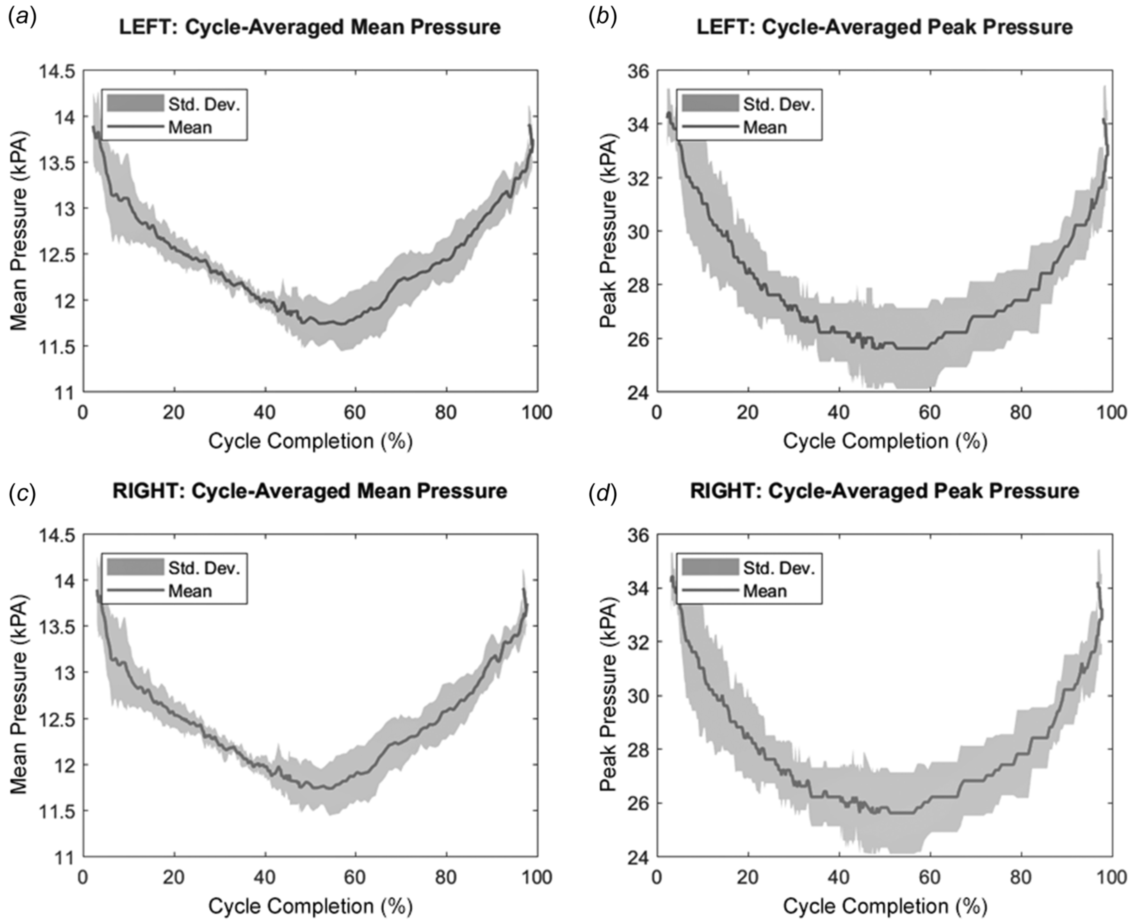

Figure 6 Magnitude of cycle-averaged interfacial pressure [kPa] as a function of cycle completion [%] during a leg press, depicting the (*a*) spatial mean of the left leg, the (*b*) peak element pressure for the left leg, the (*c*) spatial mean of the right leg, and the (*d*) peak element pressure for the right leg

Appendix C: Optimal Support Geometry Data

Table 1 Optimal backrest geometry based on peak minimization for all subjects (N = 12) that performed a trial on backrest profiles containing a centrally positioned prominence (P = 9.4, 18.9, 28.3 cm)

Gender G	Age A (years)	Height H (cm)	Mass M (Kg)	Support position P (mm)	Support depth D (mm)	Norm. mean pressure m_n	Norm. mean Std. Dev. σ_{mn}	Norm. peak pressure p_n	Norm. peak Std. Dev. σ_{pn}
Individual data									
F	32	159.0	61	94.8	7	1.05	0.02	0.91	0.07
F	25	163.0	57	284.3	7	0.96	0.04	0.80	0.05
F	22	164.0	53	93.8	21	0.84	0.02	0.79	0.04
F	21	167.0	62	93.8	7	0.93	0.03	0.97	0.02
F	25	168.0	53	284.3	14	1.03	0.08	0.93	0.03
F	22	173.0	68	284.3	7	0.97	0.04	0.87	0.03
M	29	161.0	58	189.2	14	0.88	0.01	0.71	0.02
M	22	175.5	75	93.8	7	1.00	0.02	0.95	0.01
M	24	177.0	84	93.8	21	0.87	0.01	0.89	0.02
M	25	179.5	81	284.3	7	0.94	0.05	0.98	0.05
M	23	182.5	85	93.8	14	0.85	0.02	0.77	0.07
M	21	183.5	86	284.3	14	0.93	0.06	0.85	0.07
Intersubject means and standard deviations									
Means	24	171.1	69	N/A	N/A	0.94	N/A	0.87	N/A
Std. Dev.	3.2	8.2	12	N/A	N/A	0.06	N/A	0.08	N/A

Table 2 Optimal backrest geometry based on peak minimization for subjects (N = 8) that that performed a trial on all backrest profiles considered in this study

Gender G	Age A (years)	Height H (cm)	Mass M (Kg)	Support position P (mm)	Support depth D (mm)	Norm. mean pressure m_n	Norm. mean Std. Dev. σ_{mn}	Norm. peak pressure p_n	Norm. peak Std. Dev. σ_{pn}
Individual data									
F	22	164.0	53	93.8	21	0.84	0.02	0.79	0.04
F	21	167	62	45.3	7	0.90	0.03	0.79	0.05
F	25	168	53	331.3	7	0.80	0.03	0.70	0.13
F	22	173	68	45.3	7	0.84	0.03	0.67	0.01
M	22	175.5	75	45.3	21	0.94	0.05	0.86	0.07
M	24	177	84	331.3	21	0.89	0.04	0.65	0.09
M	22	182.5	85	45.3	14	0.91	0.02	0.63	0.03
M	21	183.5	86	331.3	14	0.83	0.05	0.84	0.04
Intersubject means and standard deviations									
Means	22	174	71	N/A	N/A	0.84	N/A	0.74	N/A
Std. Dev.	1.3	6.7	13	N/A	N/A	0.05	N/A	0.08	N/A

Appendix D: Mean Normalized Peak Pressure for Various Backrest Geometries

Table 3 Evaluation the mean normalized peak pressure of tested backrest geometries relative to the control geometry (flat profile) using the Wilcoxon test

Support position P (mm)	Support depth D (mm)	Number of participants n	Mean intersubject norm. peak pressure $\bar{p}_n$	Standard error *s.e.*	Wilcoxon test statistic *W-Statistic*
0	0	11	1.00	0.03	N/A
0	0	12	1.00	0.03	N/A
45	7	11	0.92	0.05	15
45	14	11	0.95	0.07	23
45	21	11	0.94	0.06	23
94	7	12	0.98	0.04	31
94	14	12	1.06	0.04	14
94	21	12	1.07	0.05	12
189	7	12	1.03	0.04	19
189	14	12	1.11	0.06	13
189	21	12	1.11	0.06	10
284	7	12	1.01	0.04	17
284	14	12	1.10	0.05	11
284	21	12	1.07	0.04	6
331	7	11	0.91	0.04	10
331	14	11	1.00	0.05	32
331	21	11	1.08	0.10	24

Note: Not all participants made themselves available for testing on every occasion which resulted in a discrepancy in the number of participants tested for each geometry ($n = 12$ or $n = 11$). As such, the test statistic for a two-tailed Wilcoxon test using $\alpha = 0.05$ is $W_{crit} = 14$ when n = 12, and $W_{crit} = 10$ when $n = 11$.

References

[1] Duthey, B., and WHO, 2013, "Background Paper 6.24 Low Back Pain," No. 6–24, pp. 0–29.

[2] Kell, R. T., and Asmundson, G. J. G., 2009, "A Comparison of Two Forms of Periodized Exercise Rehabilitation Programs in the Management of Chronic Nonspecific Low-Back Pain," J. Strength Cond. Res., **23**(2), pp. 513–523.

[3] Kristensen, J., and Franklyn-Miller, A., 2012, "Resistance Training in Musculoskeletal Rehabilitation: A Systematic Review," Br. J. Sports Med., **46**(10), pp. 719–726.

[4] Tjøsvoll, S. O., Mork, P. J., Iversen, V. M., Rise, M. B., and Fimland, M. S., 2020, "Periodized Resistance Training for Persistent Non-Specific Low Back Pain: A Mixed Methods Feasibility Study," BMC Sports Sci. Med. Rehab., **12**, pp. 1–12.

[5] Aasa, U., Svartholm, I., Andersson, F., and Berglund, L., 2017, "Injuries Among Weightlifters and Powerlifters: A Systematic Review," Br. J. Sports Med., **51**(4), pp. 211–219.

[6] Padulo, J., Migliaccio, G., Ardigò, L., Leban, B., Cosso, M., and Samozino, P., 2017, "Lower Limb Force, Velocity, Power Capabilities During Leg Press and Squat Movements," Int. J. Sports Med., **38**(14), pp. 1083–1089.

[7] Bush, T. R., and Hubbard, R. P., 2007, "Support Force Measures of Midsized Men in Seated Positions," ASME J. Biomech. Eng., **129**(1), pp. 58–65.

[8] Rosen, J., and Arcan, M., 2003, "Modeling the Human Body/Seat System in a Vibration Environment," ASME J. Biomech. Eng., **125**(2), pp. 223–231.

[9] Zenk, R., Franz, M., Bubb, H., and Vink, P., 2012, "Technical Note: Spine Loading in Automotive Seating," Appl. Ergon., **43**(2), pp. 290–295.

[10] Zemp, R., Taylor, W. R., and Lorenzetti, S., 2013, "In Vivo Spinal Posture During Upright and Reclined Sitting in an Office Chair," Biomed. Res. Int., **2013**, Article No. 916045, pp. 2–6.

[11] Zemp, R., List, R., Gülay, T., Elsig, J. P., Naxera, J., Taylor, W. R., and Lorenzetti, S., 2014, "Soft Tissue Artefacts of the Human Back: Comparison of the Sagittal Curvature of the Spine Measured Using Skin Markers and an Open Upright MRI," PLoS One, **9**(4), pp. e95426–e95428.

[12] Gruevski, K. M., Holmes, M. W. R., Gooyers, C. E., Dickerson, C. R., and Callaghan, J. P., 2016, "Lumbar Postures, Seat Interface Pressures and

Discomfort Responses to a Novel Thoracic Support for Police Officers During Prolonged Simulated Driving Exposures," Appl. Ergon., **52**, pp. 160–168.
[13] B, T., and A, M., 2000, "Modeling the Body/Chair interaction - An Integrative Experimental- Numerical Approach," Clin. Biomech., **15**(3), pp. 217–219.
[14] Wan, Y., and Schimmels, J. M., 1997, "Optimal Seat Suspension Design Based on Minimum ''Simulated Subjective Response," ASME J. Biomech. Eng., **119**(4), pp. 409–416.
[15] Coleman, N., Hull, B. P., and Ellitt, G., 1998, "An Empirical Study of Preferred Settings for Lumbar Support on Adjustable Office Chairs," Ergonomics, **41**(4), pp. 401–419.
[16] Flück, M., Bosshard, R., and Lungarella, M., 2017, "Cardiovascular and Muscular Consequences of Work-Matched Interval-Type of Concentric and Eccentric Pedaling Exercise on a Soft Robot," Front. Physiol., **8**, p. 640.
[17] Chrif, F., Nef, T., and Hunt, K. J., 2018, "Investigation of Cardiopulmonary Exercise Testing Using a Dynamic Leg Press and Comparison With a Cycle Ergometer," BMC Sports Sci. Med. Rehab., **10**(5), pp. 1–11.
[18] Fitze, D. P., Franchi, M., Popp, W. L., Ruoss, S., Frey, W. O., and Flück, M., 2019, "Concentric and Eccentric Pedaling-Type Interval Exercise on a Soft Robot for Stable Coronary Artery Disease Patients: Toward a Personalized Protocol Corresponding Author:," JMIR Res. Protoc., **8**, pp. 1–14.
[19] FESTO, "Fluidic Muscle DMSP/MAS," 2008, *Technical Specifications*. June.
[20] Dynamic Devices AG, "DD System Pro.," 2019, *Technical Specifications*. May.
[21] Dynamic Devices AG, "Train with a Robot," 2019, *Technology White Paper*. Mar.
[22] Novel Gmbh AG, "S2073 Pressure Sensor Mat," 2010, *Technical Specifications*. Oct.
[23] Rasmussen, J., Tørholm, S., and de Zee, M., 2009, "Computational Analysis of the Influence of Seat Pan Inclination and Friction on Muscle Activity and Spinal Joint Forces," Int. J. Ind. Ergon., **39**(1), pp. 52–57.
[24] Zemp, R., Taylor, W. R., and Lorenzetti, S., 2015, "Are Pressure Measurements Effective in the Assessment of Office Chair Comfort/Discomfort? A Review," Appl. Ergon., **48**, pp. 273–282.
[25] Driscoll, C., Aubin, C. E., Labelle, H., and Dansereau, J., 2008, "The Relationship Between Hip Flexion/Extension and the Sagittal Curves of the Spine," Stud. Health Technol. Inform., **140**, pp. 90–95.
[26] Stephens, G. C., Yoo, J. U., and Wilbur, G., 1996, "Lumbar Alignment for Different Operative Positions.pdf," Spine, **21**(15), pp. 1802–1806.
[27] Hayden, A. M., Hayes, A. M., Brechbuhler, J. L., Israel, H., and Place, H. M., 2018, "The Effect of Pelvic Motion on Spinopelvic Parameters," Spine J., **18**(1), pp. 173–178.
[28] Guo, L.-X., Dong, R.-C., and Zhang, M., 2016, "Effect of Lumbar Support on Seating Comfort Predicted by a Whole Human Body-Seat Model," Int. J. Ind. Ergon., **53**, pp. 319–327.
[29] Ribeiro, A. S., Avelar, A., Schoenfeld, B. J., Trindade, M. C. C., Ritti-Dias, R. M., Altimari, L. R., and Cyrino, E. S.,.2014, "Effect of 16 Weeks of Resistance Training on Fatigue Resistance in Men and Women," J. Hum. Kinet.,**42**(1), pp. 165–174.
[30] Sundstrup, E., Jakobsen, M. D., Brandt, M., Jay, K., Aagaard, P., and Andersen, L. L., 2016, "Strength Training Improves Fatigue Resistance and Self-Rated Health in Workers With Chronic Pain: A Randomized Controlled Trial," BioMed Res. Int., **2016**, pp. 1–11.
[31] Fiogbe, E., Carnavale, B. F., and Takahashi, A. C. D M., 2019, "Exercise Training in Older Adults, What Effects on Muscle Control? A Systematic Review of Randomized Clinical Trials," Arch. Gerontol. Geriatr., **83**, pp. 138–150.
[32] Carroll, T. J., Riek, S., and Carson, R. G., 2001, "Neural Adaptations to Resistance Training: Implications for Movement Control," Sport. Med., **31**(12), pp. 829–840.